

AD-

This report may be released to OIS.



RESEARCH LABORATORY

# ESTIMATING METAL PARTICLE COMBUSTION KINETICS

BY

R. W. BARTLETT  
J. N. ONG, JR.  
W. M. FASSELL, JR.  
C. A. PAPP

2 JULY 1962



**AERONUTRONIC**

AERONUTRONIC DIVISION • FORD MOTOR COMPANY

FORD ROAD/NEWPORT BEACH, CALIFORNIA

CLEARINGHOUSE FOR FEDERAL SCIENTIFIC AND TECHNICAL INFORMATION

Loan Document Processing Record

Accession No. AD 614/563

Date received                      1965  
by Input  
Date due out May 12  
from Input

THIS DOCUMENT IS ON LOAN

Please fill in date and sign when each action below has been completed.

	<u>Date</u>	<u>Signature</u>
Film for Microfiche	<u>5-21-65</u>	<u>[Signature]</u>
Film for Prestock or Restock	<u>                    </u>	<u>                    </u>
Report Returned to Input	<u>                    </u>	<u>                    </u>
Document Returned to Sender	<u>                    </u>	<u>                    </u>

**CLEARINGHOUSE FOR FEDERAL SCIENTIFIC AND TECHNICAL INFORMATION, CPSTI  
INPUT SECTION 410.11**

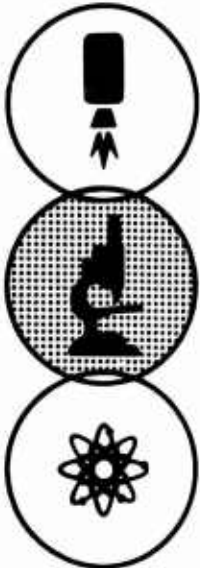
**LIMITATIONS IN REPRODUCTION QUALITY OF TECHNICAL ABSTRACT BULLETIN  
DOCUMENTS, DEFENSE DOCUMENTATION CENTER (DDC)**

*AD-614563*

- 1. AVAILABLE ONLY FOR REFERENCE USE AT DDC FIELD SERVICES.  
COPY IS NOT AVAILABLE FOR PUBLIC SALE.
- 2. AVAILABLE COPY WILL NOT PERMIT FULLY LEGIBLE REPRODUCTION.  
REPRODUCTION WILL BE MADE IF REQUESTED BY USERS OF DDC.
  - A. COPY IS AVAILABLE FOR PUBLIC SALE.
  - B. COPY IS NOT AVAILABLE FOR PUBLIC SALE.
- 3. LIMITED NUMBER OF COPIES CONTAINING COLOR OTHER THAN BLACK  
AND WHITE ARE AVAILABLE UNTIL STOCK IS EXHAUSTED. REPRODUCTIONS  
WILL BE MADE IN BLACK AND WHITE ONLY.

TSL-121-2/64

DATE PROCESSED: *5/10/65*  
PROCESSOR: *F. Q. J.*



RESEARCH LABORATORY

# ESTIMATING METAL PARTICLE COMBUSTION KINETICS

BY

R. W. BARTLETT  
J. N. ONG, JR.  
W. M. FASSELL, JR.  
C. A. PAPP

2 JULY 1962

THE WORK DESCRIBED HEREIN WAS SPONSORED BY THE  
ADVANCED RESEARCH PROJECTS AGENCY THROUGH THE  
BUREAU OF NAVAL WEAPONS UNDER CONTRACT NOw 61-0905-c



**AERONUTRONIC**

AERONUTRONIC DIVISION • FORD MOTOR COMPANY

FORD ROAD / NEWPORT BEACH, CALIFORNIA

## ABSTRACT

A combustion model for metal particles is derived and compared with experimental results for a few metals with high combustion enthalpies. It is concluded that aluminum and beryllium oxidize slowly because of formation of solid oxide films which impede the transport of reactants at temperatures below their oxide melting points. Diffusion through the liquid oxides is several decades faster, causing ignition to occur at the oxide melting point. After ignition, the temperature rises rapidly. When the metal boiling point is reached, metal evaporation expands the liquid oxide shell until the evaporation rate and rate of diffusion of reactant through the oxide shell are equal. The oxidation reaction occurs at the oxide shell rather than the metal interface and proceeds by this mechanism until the particle is consumed. Expansion of this shell accounts for the prevalence of hollow oxide spheres observed in the quenched combustion products. Calculations of the elapsed times for each stage in the combustion sequence have been machine computed. Inadequate knowledge about diffusion coefficients in liquid oxides is the principal uncertainty involved. The diffusion flame theory adequately accounts for the combustion of magnesium.

## NOMENCLATURE

- $C$  = reactant concentration ( $\text{g cm}^{-3}$ )  
 $\Delta C$  = concentration difference across diffusion barrier ( $\text{g cm}^{-3}$ )  
 $\bar{C}_P$  = heat capacity at constant pressure, per unit mass ( $\text{cal/g}^\circ\text{K}$ )  
 $d$  = effective gas molecule collision diameter (cm)  
 $D_0$  = initial particle diameter (cm)  
 $D_{12}$  = diffusion coefficient of reactant species in liquid oxide ( $\text{cm}^2 \text{sec}^{-1}$ )  
 $\Delta F^\ddagger$  = activation free energy (kcal/mole)  
 $g$  = acceleration of gravity ( $980 \text{ cm sec}^{-2}$ )  
 $h$  = heat transfer coefficient ( $\text{cal cm}^{-2} \text{sec}^{-1} \text{ }^\circ\text{K}^{-1}$ )  
 $h$  = Planck's constant  
 $k$  = Boltzmann constant  
 $k$  = thermal conductivity ( $\text{cal cm}^{-1} \text{s}^{-1} \text{ }^\circ\text{K}^{-1}$ )  
 $k_0$  = conversion constant  
 $k_1 = W_r \bar{C}_{Pv} / 4 \pi k_v$  (cm)  
 $K$  = ratio of  $R_m / R_1$   
 $m$  = mass of metal oxidized (g)  
 $M$  = molecular weight  
 $q$  = heat flux ( $\text{cal cm}^{-2} \text{sec}^{-1}$ )

- $Q_v$  = total rate of heat flow to metal sphere from metal vapor ( $\text{cal sec}^{-1}$ )
- $r$  = radius of isothermal contours (cm)
- $R$  = gas constant
- $R$  = particle radius (cm)
- $R_1$  = inner radius of oxide shell (cm)
- $R_2$  = outer radius of oxide shell (cm)
- $t$  = time (sec)
- $T$  = temperature ( $^{\circ}\text{K}$ )
- $V_{\infty}$  = hot gas streaming velocity ( $\text{cm sec}^{-1}$ ) relative to particle
- $V_r$  = metal vapor diffusion velocity, radial direction
- $W_r$  = mass transfer rate  $\frac{dm}{dt}$  ( $\text{g sec}^{-1}$ )
- $T_{BP}$  = metal boiling point ( $^{\circ}\text{K}$ )
- $\alpha$  = thermal diffusivity ( $\text{cm}^2 \text{ s}^{-1}$ )
- $\Delta H_{fus}$  = latent heat of metal fusion (cal/g)
- $\Delta H_{vap}$  = latent heat of metal vaporization (cal/g)
- $\Delta H_{T_i}^{\circ}$  = enthalpy of metal at ignition temperature (cal/g)
- $\Delta H_{T_{BP}}^{\circ}$  = enthalpy of liquid metal at boiling point (cal/g)
- $\Delta H_f$  = heat of formation of metal oxide ( $\text{cal g}^{-1}$  of metal)
- $\mu$  = gas viscosity (poise)
- $\rho_m$  = metal density ( $\text{g cm}^{-3}$ )
- $\rho_i$  = oxide density
- $\sigma$  = Stefan Boltzmann constant

### Subscripts

- c = metal oxide
- f = gas film adjacent to metal particle
- g = gas or flame
- i = ignition
- m = metal or metal surface
- o = initial condition
- v = metal vapor
- v = radiation

## CONTENTS

	PAGE
INTRODUCTION. . . . .	1
EXPERIMENTAL SYNOPSIS . . . . .	3
COMBUSTION MODEL. . . . .	8
IGNITION DELAY	
Thermal Flux Calculation. . . . .	15
Heat Conduction and Temperature Increase Within the Particle. . . . .	20
Delay Due to Latent Heat of Fusion. . . . .	22
Comparison With Experimental Results. . . . .	24
COMBUSTION AT ATMOSPHERIC PRESSURE WITHOUT METAL EVAPORATION. . . .	26
METAL EVAPORATION AND EXPANSION OF THE OXIDE SHELL	
Analysis. . . . .	31
Results . . . . .	37
DISCUSSION. . . . .	41
REFERENCES. . . . .	43

## ILLUSTRATIONS

FIGURE		PAGE
1	Cross Section of Aluminum Alloy Combustion Products Showing Spherical Oxide Shells. . . . .	5
2	Admixture of 65 Percent Al and 35 Percent Mg Burning in Oxygen Natural Gas . . . . .	6
3	Schematic Plot of Metal and Oxide Temperatures and Metal Droplet Radius during the Three Combustion Stages . . .	13
4	Computed Ignition Delay in a Metallized Flame . . . . .	23
5	$\tau_{del}$ for Combustion with Metal Evaporation and Expansion of the Liquid Oxide Shell . . . . .	32
6	Regression of Radius during Combustion of 100-Micron Spheres of Aluminum using Evaporation Model; System Pressure One Atmosphere; $T_A = 3700^\circ\text{K}$ . . . . .	38
7	Regression of Radius during Combustion of 100-Micron Spheres of Beryllium using Evaporation Model; System Pressure One Atmosphere; $T_A = 3900^\circ\text{K}$ . . . . .	39

## INTRODUCTION

Most of the studies of heterogeneous combustion have assumed that the combustion reaction occurs in the gas phase, forming a spherical diffusion flame around the fuel droplet. This theory has been summarized by Penner<sup>1</sup> and adequately accounts for the combustion of magnesium.<sup>2</sup> However, experience with higher boiling metals has indicated that their behavior does not conform to the diffusion flame theory.<sup>2-4</sup> It has long been recognized by Vulis and other Russian investigators that the combustion of carbon cannot occur by a gas phase reaction but must occur at the particle or pore surface.<sup>5</sup> They have observed that, depending on the flow and thermal regimes, the combustion rate will be controlled by either diffusion of oxygen or product gas species to or away from the surface or by the rate of chemical reaction at the surface.

Only metals with high oxide formation enthalpies are attractive energy sources and as a result their oxides are invariably stable condensed phases at high temperatures. When this situation is coupled with

a moderately high metal boiling point, the slow and rate controlling step may shift to transport of reactants through the oxide layer. Aluminum and beryllium are believed to be examples of this mode of combustion. The correlation of minimum aluminum ignition temperature with the melting point of  $\text{Al}_2\text{O}_3$  has been observed by Friedman and Macek.<sup>6</sup> This study is principally concerned with the analysis of this latter type of combustion. A combustion model is presented and the results calculated from it are compared with the available experimental data on aluminum and beryllium.

## EXPERIMENTAL SYNOPSIS

Burning times were determined by photographing the incandescent particles in a methane-oxygen torch using a high speed motion picture camera or a still plate camera in combination with a rotating light chopper.<sup>7</sup> The particles travelled in the same direction as the flame and ignition delay times were approximated by dividing the measured distance of the hot zone of the flame through which the particle travelled before igniting, by the particle velocity. The pre-ignition particle velocity was assumed to be the same as the post-ignition velocity determined by the motion picture camera or chopper. The sharp transition of the particle from nonluminous to brilliant incandescence was used to indicate ignition. Observations were made on aluminum, magnesium, beryllium, zirconium, titanium, niobium, tantalum, silicon, chromium, iron and various alloys of these metals. The principal qualitative results are summarized below. The quantitative results are compared with predicted results later.

- (1) All of the metals but beryllium and large aluminum and silicon particles ignited and burned in the torch.
- (2) With the exception of magnesium, the combustion products included as a major constituent hollow spheres about the same size as the original particle, Figure 1. Propellant strand burning tests also produced hollow spheres.
- (3) The MgO particles were much smaller, usually less than one micron, and often appeared as single crystals. Magnesium-aluminum alloys with a magnesium content greater than 20% also burn in this manner. The difference between magnesium and aluminum particle combustion is illustrated by Figure 2, which shows a mixture of aluminum and magnesium particles burning in a torch flame. The luminous cloud is characteristic of magnesium. The sharp light spots are individual aluminum particles.



FIGURE 1. CROSS SECTION OF ALUMINUM ALLOY COMBUSTION PRODUCTS  
SHOWING SPHERICAL OXIDE SHELLS

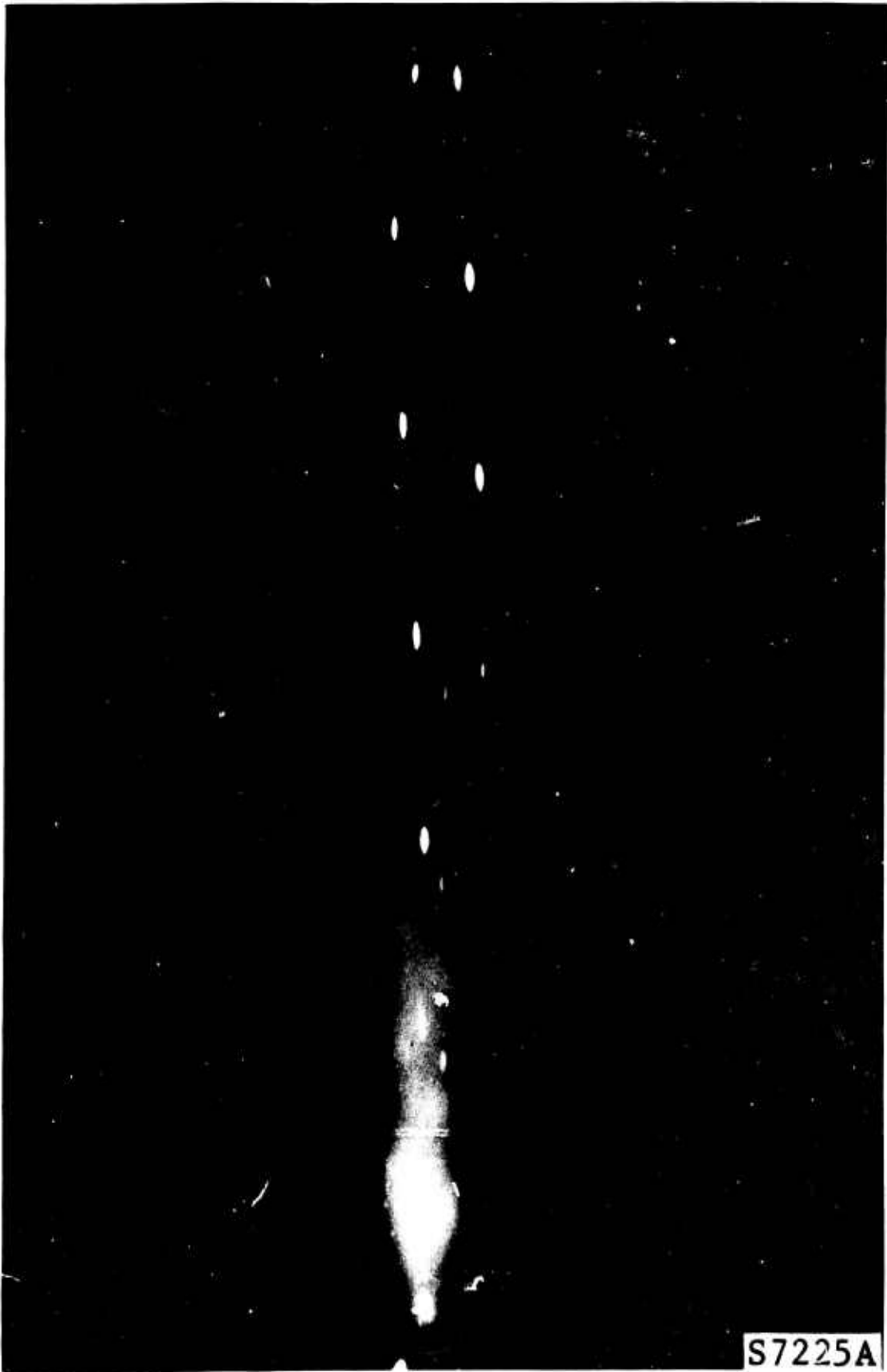


FIGURE 2. MIXTURE OF -115 +150 MESH ALUMINUM AND MAGNESIUM PARTICLES BURNING IN AN OXYGEN-NATURAL GAS FLAME; PHOTOGRAPHED THROUGH A 160-INTERRUPTIONS-PER-SECOND LIGHT CHOPPER

(4) Starring, attributed to fragmentation, and spiral motion of some metals and alloys were often observed.

Any successful analysis of metal particle combustion kinetics must predict the burning times with some reasonable degree of accuracy, provide for reasonable agreement with observed ignition temperatures and explain the formation of hollow oxide spheres.

## COMBUSTION MODEL

Heat and mass transfer problems usually can be solved only for simple geometric shapes and all of the calculations presented here are based on spherical geometry. The melting points of most metals with high oxidation enthalpies are on the lower end of the combustion temperature range, 300°K to > 3000°K. Since surface tension will cause the liquid metal to assume a spherical shape, an error due to the assumption of spherical geometry for nonspherical particles will only exist during a brief initial period.

Before presenting the method of calculation, a review of the model on which it is based is necessary. For a metal sphere at an initial low temperature  $T_0$ , injected into a hot gas stream or flame at temperature  $T_g$ , the oxidation rate will depend on the surface temperature and mechanism of oxidation. For many metals, including aluminum and beryllium, the oxidation rates are believed to be controlled by diffusion of reacting ions through the solid oxide coating<sup>8,9</sup> that is

formed. The rate is relatively slow as long as the oxide remains solid. Diffusion rates in liquids are much faster than in solids. The increase is several orders of magnitude<sup>10</sup> and the oxidation rate will increase correspondingly at the oxide melting point. Consequently, for this type of system, ignition is expected to occur at the melting point of the oxide,  $T_i$ .

The oxide coating formed on magnesium is not adherent and does not act as an effective diffusion barrier. Oxygen gas can pass directly to the metal surface. Provided oxygen diffusion through the gas boundary layer is not limiting, the rate of oxidation of this type of metal depends on the surface reaction rate and increases exponentially with temperature,

$$\frac{dm}{dt} = C_A k_o \frac{kT}{h} e^{-\Delta F^\ddagger/RT} \quad (1)$$

As the particle is heated, a temperature is eventually reached where the thermal flux from oxidation becomes appreciable. This increases the temperature at a faster rate and very soon the temperature itself is increasing at a quasi exponential rate. For this system there will not be a precise ignition temperature but a narrow temperature band above which the oxidation rate and temperature increase sharply. An average temperature in this band is taken as the ignition temperature for this type of system. For magnesium, this has been observed to be about 900°K.<sup>11</sup>

In both cases, the heat flux and surface regression rate caused by oxidation are negligible before ignition but must be considered at higher temperatures.

Following ignition, the combustion behavior of magnesium, beryllium and aluminum differ from each other and also depend on the system pressure. Magnesium has a vapor pressure of 10 mm at 1000°K and its normal boiling point is 1381°K. Magnesium oxide is a stable solid at these temperatures and since no phase changes are involved, it is expected to remain porous and permit rapid transport of oxygen and also metal vapor. Magnesium combustion is directly related to the vaporization of magnesium. Although a direct gas phase reaction to produce MgO vapor is not thermodynamically possible, magnesium vapor species and oxygen can react on surfaces to produce solid MgO. As a result, very small MgO crystals quickly nucleate and grow in the surrounding gas, accounting for the luminous cloud and small crystals that are observed in burning experiments. The combustion rate is dependent on the evaporation rate which depends on the heat flux to the metal particle.

The behavior of aluminum, beryllium and many other metals is quite different from magnesium even above their ignition points. As a result, longer periods are required to complete combustion and an analysis of the kinetic process is warranted. Above the ignition temperature, aluminum and beryllium are covered with molten oxide layers which prevent

metal evaporation provided the vapor pressure of the metal is less than the system pressure. The normal metal boiling point and oxide melting point of beryllium are almost the same. The temperature of aluminum must be raised from 2300°K to 2740°K for boiling to occur. In both cases, once the boiling point is attained, metal evaporation will expand the oxide shell providing a metal vapor envelope between the metal sphere and the oxide shell. It is important to emphasize that diffusion through the liquid oxide shell is still slow when compared with gaseous diffusion and reaction will occur at the oxide shell rather than at individual nuclei in the surrounding gas. The oxide shell will expand or contract to permit the mass rate of metal evaporated from the metal sphere to equal the rate of oxidation of metal at the oxide. Any sudden ejection of the particle from the hot zone quickly freezes the oxide shell and accounts for the hollow oxide spheres with contained metal particles which have been collected, sectioned and observed microscopically. Such particles are very numerous in most combustion experiments.

In any practical thermodynamic application, the chamber pressure must be much higher than one atmosphere, and as a result, the metal boiling points will increase. The extrapolation of vapor pressure data taken at temperatures below 1700°K to temperatures above the normal boiling points is very hazardous. In lieu of better information, however, such an extrapolation indicates a boiling point of about 3450°K for both aluminum and beryllium at 1000 psi. As the chamber pressure and boiling

point increase, the thermal gradient causing evaporation will decrease and the combustion time will increase. At sufficiently high pressures, no evaporation can occur.

It is convenient to separate the combustion of metals which behave in the manner of aluminum and beryllium into three consecutive stages separated by the ignition temperature and the metal boiling point and compute the elapsed time for each stage. The three stages are shown schematically in Figure 3 and summarized in Table I. The sum of these elapsed times gives the time interval required for complete combustion to occur. All calculations are based on assumed flame temperatures of  $3300^{\circ}\text{K}$  for aluminum,  $3450^{\circ}\text{K}$  for beryllium and  $3150^{\circ}\text{K}$  for magnesium.

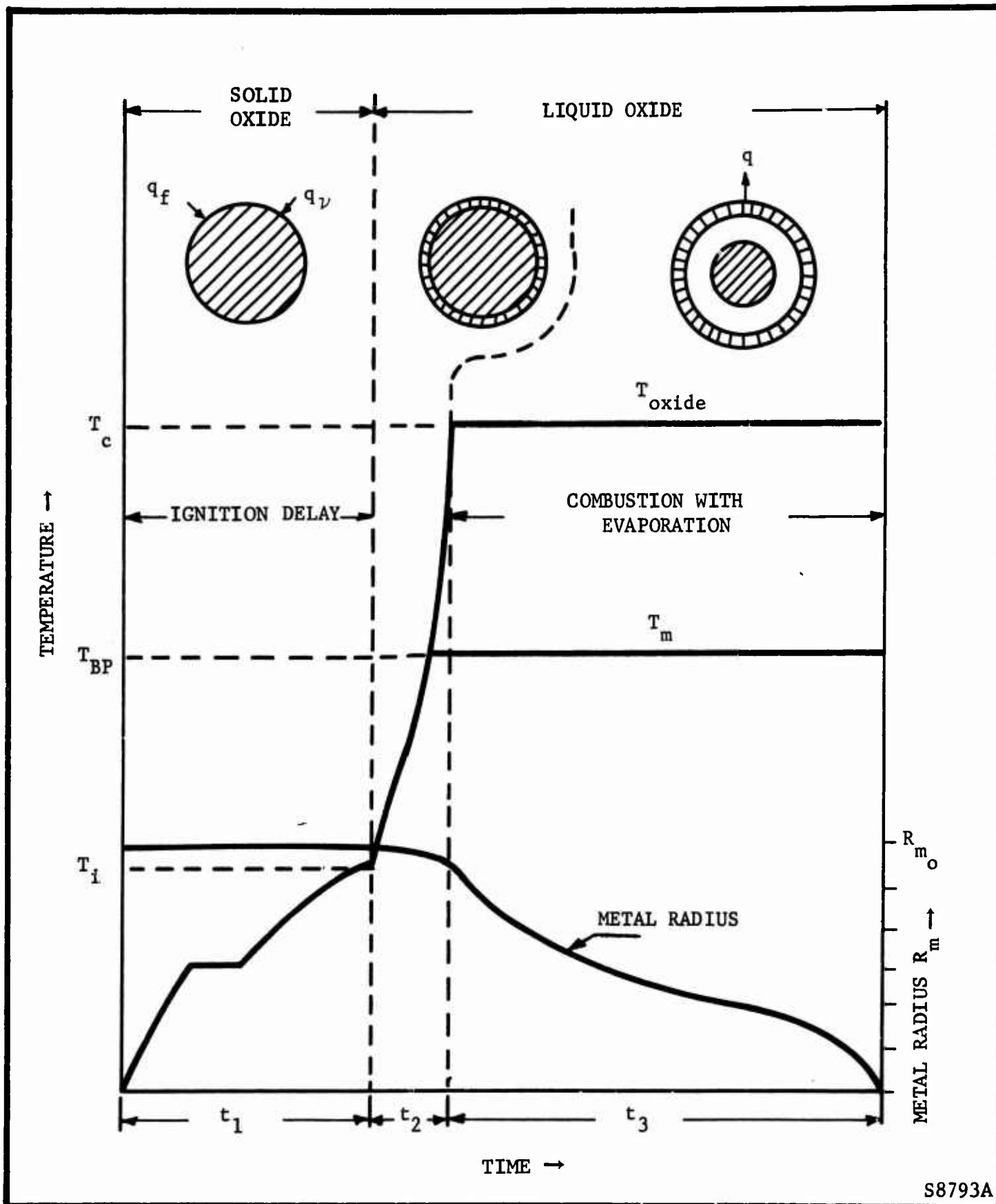


FIGURE 3. SCHEMATIC PLOT OF METAL AND OXIDE TEMPERATURES AND METAL DROPLET RADIUS DURING THE THREE COMBUSTION STAGES

TABLE I

SUMMARY OF COMBUSTION CHARACTERISTICS OF ALUMINUM AND BERYLLIUM

<u>Combustion Stage</u>	<u>Temperature Limits</u>	<u>Controlling Parameters</u>	<u>Calculations of Elapsed Times</u>
1. Ignition Delay	Initial Temperature to Oxide Melting Point	(1) Convective Heat Flux - Major Thermal Source.  (2) Radiation - Minor Thermal Source.  (3) Heat from Reaction, Neglected.  (4) Oxidation Slow because of Oxide Film Diffusion Barrier.	Equation (14)
2. Combustion Without Evaporation (Al at Low Pressures Only).	Oxide Melting Point to Metal Boiling Point	(1) Convective Heat Flux - Major Source.  (2) Heat from Reaction - Major Source.	Equation (24)
3. Metal Evaporation and Expansion of the Oxide Shell.	Metal Remains at BP. Oxide Steadies at Higher Temp. which gives Thermal Flux Balance.	(1) Heat Transfer by Conduction and Transpiration from Oxide Shell to Metal Droplet.  (2) Metal Vapor Expands Oxide Shell.  (3) Oxidation Diffusion Controlled Through Shell.	Equations (33) and (35).

## IGNITION DELAY

### Thermal Flux Calculation

The thermal flux to the metal during the period prior to ignition is the sum of convection and radiation from the surroundings. During this period the oxidation reaction is a negligible thermal source. The convective flux,  $q_f$ , across the gas boundary film can be calculated,

$$q_f = h_f (T_g - T_m) \quad (2)$$

using the Nusselt number

$$Nu = \frac{h_f D_o}{k_f} \quad (3)$$

The following correlations for forced and free convection were taken from Ranz and Marshall.<sup>13</sup> For high streaming velocities, the Nusselt number depends on the Reynolds and Prandtl numbers:

$$\frac{h_f D_o}{k_f} = 2.0 + 0.60 \left( \frac{D_o v_\infty \bar{\mu}_f}{\mu} \right)^{1/2} \left( \frac{\bar{C}_p \mu}{k} \right)_f^{1/3} \quad (4)$$

For free convection the Nusselt number depends on the Grashof number,

$$\left[ \frac{D_o^3 \bar{\rho}_f^2 g \Delta T_f}{\mu^2 \bar{T}_f} \right], \text{ and Prandtl number:}$$

$$\frac{h_f D_o}{k_f} = 2.0 + 0.60 \left[ \frac{D_o^3 \bar{\rho}_f^2 g \Delta T_f}{\mu^2 \bar{T}_f} \right]^{1/4} \left[ \frac{\bar{C}_p \mu}{k} \right]^{1/3} \quad (5)$$

The streaming velocity of the hot gases over a metal particle is unknown and probably varies from a low value corresponding to free convection to the flame velocity relative to the combustion chamber. The latter velocity is also a variable quantity depending on the relative location in the flame and whether the flame configuration changes with time. The thermal flux will be lowest and the ignition delay longest for free convection and calculations based on the free convection assumption will be more conservative than arbitrarily assuming an average streaming velocity. The diameters of metal particle additives are of the order of 100 microns which corresponds to low Grashof numbers, Al =  $3.37 \times 10^{-3}$ , Be =  $3.17 \times 10^{-3}$  and Mg =  $4.52 \times 10^{-3}$ . As a result, the second term in equation (5) only amounts to about 10% of the total and can be neglected. Therefore, for these systems, free convection is approximately equivalent to heat transfer from a stagnant fluid,

$$\frac{h_f D_o}{k_f} = 2$$

and from equation (2)

$$q_f = \frac{2k_f (T_g - T_m)}{D_o} \quad (6)$$

As a consequence, the convective flux is inversely proportional to the particle size.

A solution of equation (6) requires an evaluation of  $k_f$ . The prediction of thermal conductivities for polyatomic gases is only semi-empirical even for low pressure systems. Eucken's equation for thermal conductivity of polyatomic gases is:

$$k = \left[ \bar{C}_p + \frac{5R}{M} \right] \mu \quad (7)$$

A good estimate of  $k$  can be made by employing the following equation for the viscosity

$$\mu = 2.66 \times 10^{-5} \frac{\sqrt{MT}}{d^2 \Omega} \quad (8)$$

in which  $d^2$  is the collision diameter and  $\Omega$  is a dimensionless function varying slightly from unity and measures the deviation of the gas from rigid sphere behavior. The values are based on a Lennard-Jones function for the potential energy of interaction.<sup>14</sup>

For purposes of calculations, the primary combustion gases were assumed to be CO, H<sub>2</sub>O, H<sub>2</sub> and HCl in equal mole fractions. An average film thermal conductivity coefficient  $k_f^\circ$  was calculated by determining the thermal conductivity coefficient for each of these gas species using equations (7), (8) and:

$$k_{f_i} = k_{f_i}^\circ (T_f)^{1/2} \quad (9)$$

$$k_f^\circ = \frac{1}{4} \sum k_{f_i}^\circ \quad (10)$$

Dissociation of these gases may be important at high temperatures but dissociation was ignored for these initial calculations. The gas film temperature was taken as:

$$T_f = \left( \frac{T_g^{1/2} + T_m^{1/2}}{2} \right)^2$$

The values of  $k_f^\circ$  and the initial and final convective thermal fluxes for 100 micron spheres of magnesium, aluminum and beryllium are listed in Table II.

The heat flux transferred by radiation to a small sphere from a large cavity is provided by the Stephen Boltzmann law:

$$q_v = \sigma (a_m T_g^4 - e_m T_m^4) \quad (11)$$

The term  $a_g$  is the absorptivity of the metal for radiation emanating from  $T_g$ . The initial and final radiant fluxes are also listed in Table II. The values are based on estimates for effective emissivity of .20

TABLE II

PREIGNITION DELAY DATA FOR SPHERES,  $D_0 = 100$  MICRONS  
IN A METALLIZED FLAME AT THE TEMPERATURES INDICATED

		Al	Be	Mg
		<u>= 0.20</u>	<u>= 0.20</u>	<u>= 0.20</u>
$k_f^\circ$	(cal cm <sup>-1</sup> sec <sup>-1</sup> °K <sup>-3/2</sup> )	$2.36 \times 10^{-4}$	$2.44 \times 10^{-4}$	$2.30 \times 10^{-4}$
$q_f$	(cal cm <sup>-2</sup> sec <sup>-1</sup> )	5293	5870	4773
$q_f$	(cal cm <sup>-2</sup> sec <sup>-1</sup> )	2432	1509	4354
$q$	(cal cm <sup>-2</sup> sec <sup>-1</sup> )	32.1	38.3	27.0
$q$	(cal cm <sup>-2</sup> sec <sup>-1</sup> )	24.2	19.2	26.8
Elapsed Time to heat sphere from $T_o$ to $T_i$ (milliseconds)		0.5	1.32	0.1
Elapsed time to fuse sphere (milliseconds)		0.173	0.50	0.12
Total preignition delay (milliseconds)		0.673	1.82	0.22
Estimated flame temperature (°K)		3300	3450	3150

which is somewhat less than the average values of the total emissivities for the oxides over the preignition temperature range.<sup>15</sup> The calculations also assume  $e_m = a_m$ . The estimation of high temperature emissivities is hazardous, but the radiation flux is less than the convective flux and a 30% error in  $e_m$  will only result in a 4% to 6% error in the final elapsed time calculation.

### Heat Conduction and Temperature Increase Within The Particle

To determine the temperature increase in the sphere, the equation of heat conduction in spheres must be solved. Because the flux at the surface is geometrically uniform, isothermal surfaces within the metal are concentric spheres and the equation of heat conduction is:

$$\frac{\delta T}{\delta r} = \alpha_m \frac{1}{r^2} \frac{\delta}{\delta r} \left( \frac{r^2 \delta T}{\delta r} \right) \quad (12)$$

The flux at the surface is the sum:  $q_r + q_v$

$$q_f + q_v = -k_m \frac{\delta T}{\delta r} \quad r = R \quad (13)$$

The solution to this problem is provided by Carslaw and Jaeger<sup>16</sup> in the form of plots of  $\frac{k_m T}{Rq} - \frac{3\alpha_m t}{R^2}$  versus  $\frac{r}{R}$  for various values of  $\frac{\alpha_m t}{R^2}$

for a constant flux. Calculations of the temperature lag at the center of 100 micron spheres when the surface temperature is at the ignition point were made assuming the maximum thermal flux as the constant flux. The temperature lag for beryllium and aluminum was about 100°C. This comparatively small temperature decrease is caused by the high thermal conductivity of metals and small size of the sphere. As a result of the small temperature lag, little error will be encountered if the metal sphere is regarded as a heat sink with infinite thermal conductivity. Under this assumption, the rate of temperature rise of the surface of the metal sphere  $T_m$  is equal to the total heat transfer rate to the sphere divided by the total heat capacity:

$$\frac{dT_m}{dt} = \frac{6 k_f (T_g^{1/2} + T_m^{1/2}) (T_g - T_m) + \sigma_e T_g - \sigma_e T_m^4}{D_o \bar{C}_p \rho_m} \quad (14)$$

From equation (14) a computation of the elapsed time to heat the metal,  $T_m$ , from  $T_o$  to  $T_1$  was made with a digital computer. In doing so, the Dulong-Petit limiting heat capacity for solids was used to compute average specific heats of the metals for the temperature range  $T_o$  to  $T_1$ . The additional heat capacity of liquid metals should be included at temperatures above the metal melting point. However, the increase is usually only about 1 cal/mole or 15% and will be partially offset by the lower heat capacity between the initial temperature  $T_o$  and the Debye temperature.

### Delay Due to Latent Heat of Fusion

An additional time must be added for latent heats of fusion of the metals which melt at or below their respective ignition points.

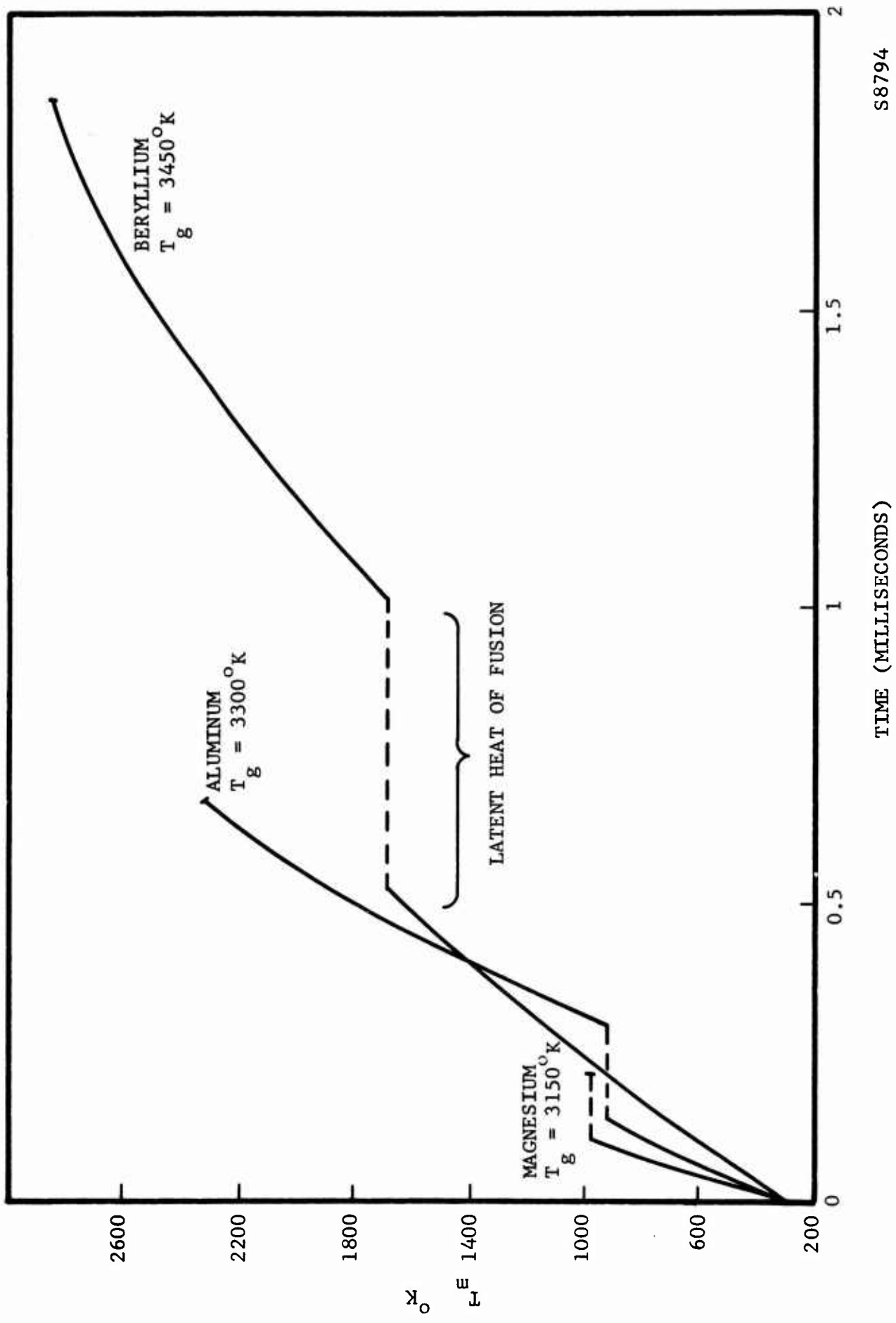
$$\frac{\Delta H_{\text{fus}} D_o \rho_m}{6} = (q_v + q_f) t \quad \left| \quad T_m = \text{M.P.} \right. \quad (15)$$

The computed elapsed times for metal sphere heating and fusion are also listed in Table II. The sum of these is the ignition delay. The temperature-time relations for this period are plotted in Figure 4.

### Effect of Particle Diameter

As shown in Table II, the heat transfer contributed by radiation is only about 1% or 2% of the total. If radiation is neglected, the elapsed time required to heat the particle to the ignition point under stagnant gas conditions is proportional to the square of the diameter. The heat required to reach  $T_i$  is:

$$\pi D_o^2 \int q_f dt = \frac{\pi D_o^3}{6} \left[ \bar{c}_{p_m} \rho_m (T_i - T_o) + \Delta H_{\text{fus}} \right] \quad (16)$$



S8794

FIGURE 4. COMPUTED IGNITION DELAY IN A METALLIZED FLAME

substituting equation (6) in equation (16) yields the parabolic relation,

$$t = \left\{ \frac{\left[ \bar{c}_{p_m} \rho_m (T_i - T_o) + \Delta H_{fus} \right]}{12 k_f (\overline{T_g - T_m})} \right\} D_o^2 \quad (17)$$

where  $(\overline{T_g - T_m})$  is an effective average temperature gradient.

#### Comparison with Experimental Results

A parabolic dependence of the time on ignition particle size has been observed by Friedman and Macek<sup>6</sup> who measured the ignition delay for aluminum spheres of various sizes using a combustion torch similar to a Meeker burner. The fuel was a propane and oxygen mixture with a calculated adiabatic flame temperature of 2510°K. For a 100 micron sphere, the ignition delay was 21 milliseconds (extrapolated).

A computation of the ignition delay for these conditions was made using equation (14). The thermal conductivity was calculated in the same manner but based on a gas consisting of 57 mole % H<sub>2</sub>O and 43 mole % CO<sub>2</sub> which reflects combustion of propane. The lower thermal conductivity, caused by the absence of low molecular weight H<sub>2</sub>, combined with the lower flame temperature, 2510°K, extend the ignition time. The computed result was 8.3 milliseconds.

Although ignition delays were not measured in this laboratory, the maximum aluminum particle size that ignited, 115 ± 10 microns, was

compared with the maximum exposure time. The latter was calculated from the particle velocity, using motion pictures, and maximum path length of the particle in the hot zone of the flame. The exposure time for a 115 micron aluminum particle varied between 15 and 20 milliseconds. The computed ignition delay for this size was 11 milliseconds.

When the hazards of estimating thermal conductivities of gases at high temperatures are considered the agreement between observed and computed ignition delay is probably satisfactory. The minimum flame temperature that would cause ignition of aluminum particles was determined by Friedman and Macek and by the authors. In both cases, the minimum flame temperature was observed to be within  $\pm 80^{\circ}\text{C}$  of the melting point of  $\text{Al}_2\text{O}_3$ .

## COMBUSTION AT ATMOSPHERIC PRESSURE WITHOUT METAL EVAPORATION

It was previously mentioned that aluminum has a normal boiling point of 2740°K while its oxide melts at a lower temperature, 2300°K. The heat flux is expected to increase considerably at 2300°K because the thermal flux contribution from the exothermic oxidation reaction, which is negligible below 2300°K, becomes a major heat source. With the addition of this heat source, the elapsed time analysis is similar to that for the ignition delay.

The oxidation rate will be limited by diffusion of reactants, either oxygen or aluminum, through the oxide layer. Specific information on diffusion in liquid  $\text{Al}_2\text{O}_3$  is not available. The diffusion coefficient varies exponentially with temperature, but for liquids the activation energy and argument of the exponent are small and the temperature effect is usually slight. As a result, virtually all liquids which do not possess abnormally high viscosities (glasses, polymers) have remarkably similar diffusion coefficients regardless of the temperature or chemical composition. The value of the diffusion coefficients are usually  $10^{-4}$  to  $10^{-5} \text{ cm}^2 \text{ sec}^{-1}$ .

The oxidation rate and associated thermal flux of aluminum decrease with increasing thickness of the liquid oxide. For thin oxide layers,  $(R_o - R_m) \ll R_o$ ,

$$\frac{dm/A}{dt} = \frac{D_{12} \Delta C}{(R_o - R_m) \frac{\rho_m}{\rho_i}} \quad (18)$$

The concentration gradient,  $\Delta C$ , depends only on the pressure, which is constant, and temperature. The oxidation rate may also be considered in relation to the spherical geometry and regression rate of the metal radius.

$$\frac{dm/A}{dt} = \frac{-dR_m}{dt} \rho_m \quad (19)$$

Substituting equation (19) in equation (18) yields

$$\frac{dr}{dt} = \frac{-D_{12} \Delta C \rho_i}{\rho_m^2 (R_o - R_m)} \quad (20)$$

which upon integrating gives

$$\frac{(R_o - R_m)^2}{2} = \frac{\rho_i D_{12} \Delta C t}{\rho_m^2} + \text{Const} \quad (21)$$

and installing the boundary conditions, at  $t = 0$ ,  $R_m = R_o$  yields:

$$(R_o - R_m) = \left[ \frac{2 \rho_i D_{12} \Delta C t}{\rho_m} \right]^{1/2} \quad (22)$$

Provided  $(R_o - R_m) \ll R_o$ , the thermal input required to heat the metal is  $(\Delta H_{T_{BP}}^\circ - \Delta H_{T_i}) \frac{4}{3} \pi R_o^3 \rho_m$ . The chemical heat source is obtained from equation (22) and consideration of the particle geometry:

$$Q_R = 4 \pi R_o^2 \left[ 2 \rho_i D_{12} \Delta C t \right]^{1/2} \overline{\Delta H_f} \quad (23)$$

where  $\overline{\Delta H_f}$  is the average heat of formation over the temperature range  $(T_{BP} - T_i)$ . For ease of calculation, the value of  $(q_v + q_f)$  at  $\frac{T_i + T_{BP}}{2}$  was used for the convective and radiant heat fluxes. The equation for the elapsed time for this period is:

$$\begin{aligned} (\Delta H_{T_{BP}}^\circ - \Delta H_{T_i}) \frac{4 \pi R_o^3}{3} \rho_m &= 4 \pi R_o^2 \left[ 2 \rho_i D_{12} \Delta C t \right]^{1/2} \overline{\Delta H_f} + \\ 4 R_o^2 t &\left\{ (q_v + q_f) \left| \left( \frac{T_i + T_{BP}}{2} \right) \right| \right\} \end{aligned} \quad (24)$$

The elapsed times calculated from equation (24) and the equivalent values of the radius regression ( $R_o - R_m$ ) are listed in Table III. Calculations were made for three values of  $D_{12} \Delta C$ ;  $10^{-4}$ ,  $10^{-5}$  and  $10^{-6}$  g cm<sup>-1</sup> sec<sup>-1</sup>.

The periods are somewhat smaller than those required for the ignition delay period in aluminum.

TABLE III

COMBUSTION OF ALUMINUM BETWEEN THE MELTING POINT  
OF  $\text{Al}_2\text{O}_3$  (2330°K) AND THE METAL BOILING POINT (2740°K)

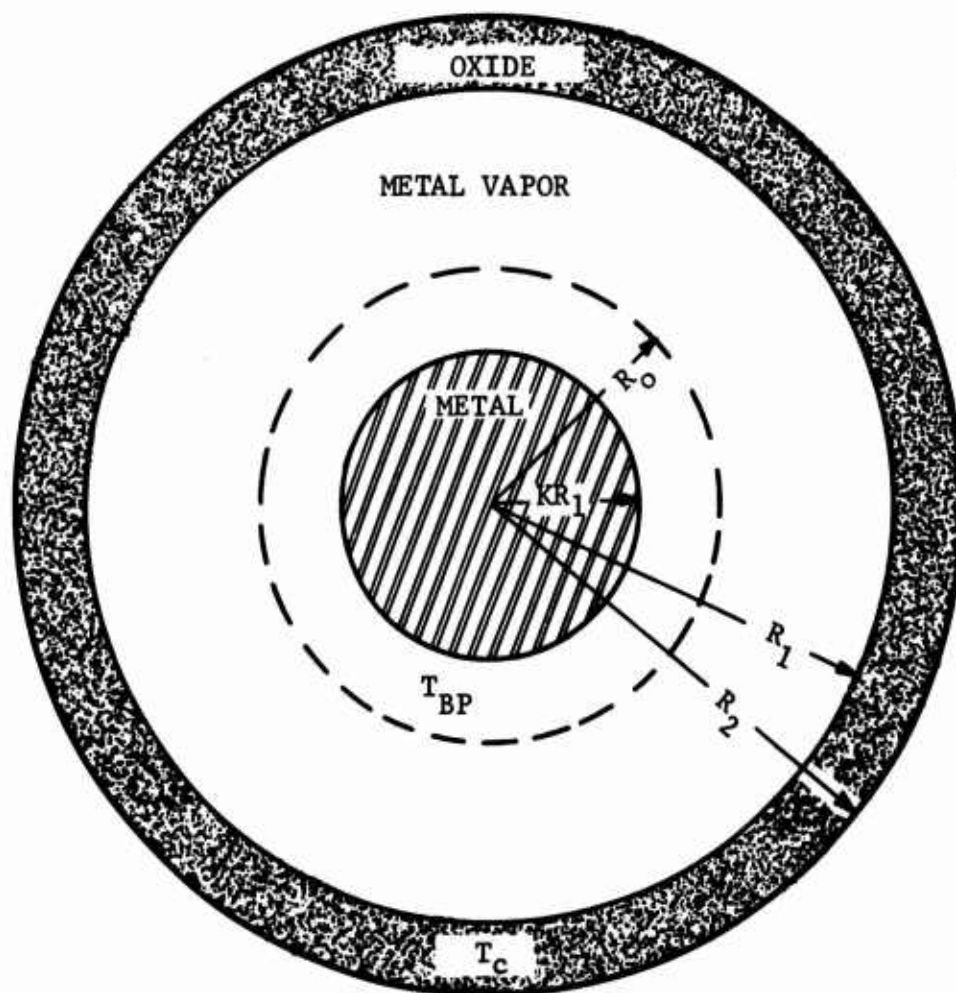
<u>Property</u>	<u><math>D_{12} \Delta C</math> (g cm<sup>-1</sup> sec<sup>-1</sup>)</u>		
	<u>10<sup>-4</sup></u>	<u>10<sup>-5</sup></u>	<u>10<sup>-6</sup></u>
$\Delta H_f$	6400 cal/g	6400 cal/g	6400 cal/g
$(\Delta H_{BP} - \Delta H_{Ti})$	115 cal/g	115 cal/g	115 cal/g
Elapsed Time (milliseconds)	.016	.085	.19
$(R_o - R_m)$ (microns)	.332	.241	.115

## METAL EVAPORATION AND EXPANSION OF THE OXIDE SHELL

### Analysis

At the boiling point, metal is evaporated from the metal sphere and transferred to the oxide shell where oxidation occurs as shown in Figure 5. The oxide shell must expand until the mass diffusion rate of reactant through the oxide is equal to the equivalent mass evaporation rate. If the evaporation rate decreases, surface tension will force the oxide shell to contract. Metal evaporates from the surface of the metal sphere at the boiling point  $T_{BP}$  and diffuses to the outer oxide shell at a higher temperature  $T_c$ . The heat removal by the sum of evaporation and transpiration of the metal vapor must maintain the sphere at  $T_{BP}$ . The mass transfer rate of the metal  $W_r$  can be expressed in terms of the radial metal vapor diffusion velocity  $V_r$

$$W_r = \frac{dm}{dt} = 4\pi r^2 \rho_v V_r \quad (25)$$



$$R_m = KR_1$$

S8795

FIGURE 5. MODEL FOR COMBUSTION WITH METAL EVAPORATION AND EXPANSION OF THE LIQUID OXIDE SHELL

It is assumed that  $V_r$  is small enough and the oxide shell sufficiently flexible that no pressure gradient occurs between the surfaces. Then the differential equation describing the temperature distribution  $T(r)$  in the space between metal sphere and oxide shell is

$$V_r \left( \frac{dT}{dr} \right) = \frac{\alpha v}{r^2} \frac{d}{dr} \left( r^2 \frac{dT}{dr} \right) \quad (26)$$

The thermal conductivity of the metal vapor is assumed constant and calculated at  $\left( \frac{T_{BP} + T_c}{2} \right)$  from the theory of monatomic dilute gases.

By substitution of equation (25) in (26)

$$\frac{dT}{dr} = \frac{4 \pi k_v}{W_r \bar{C}_{P_v}} \frac{d}{dr} \left( r^2 \frac{dT}{dr} \right) \quad (27)$$

By integrating twice and using the known boundary temperatures

we find:

$$\frac{T - T_c}{T_{BP} - T_c} = \frac{e^{-k_1/r} - e^{-k_1/R_1}}{e^{-k_1/KR_1} - e^{-k_1/R_1}} \quad (28)$$

in which  $k_1 = \frac{W_r \bar{C}_{P_v}}{4 \pi k_v}$ , and  $KR_1 = R_m$ .

The rate of heat flowing to the sphere,  $Q_v$ , required to balance the evaporation heat loss is

$$Q_v = W_r \Delta H_{\text{vap}} = -4 \pi K^2 R_1^2 q_v \Big|_{r = KR_1} \quad (29)$$

Since for spheres the heat flux is,

$$q_v = -k_v \frac{dT}{dr}$$

then by substitution in equation (29):

$$W_r \Delta H_{\text{vap}} = 4 \pi k_v K^2 R_1^2 \frac{dT}{dr} \Big|_{r = KR_1} \quad (30)$$

From equation (28) at  $r = KR_1$ ,

$$T_{\text{BP}} - T_c = e^{-k_1/KR_1} - e^{-k_1/R_1} \quad (31)$$

From this,  $\frac{dT}{dr}$  is evaluated at  $r = KR_1$  and substituted in equation (30)

to yield

$$\Delta H_{\text{vap}} = \frac{\bar{C}_{P_v} (T_c - T_{\text{BP}})}{\left\{ e^{\left[ \frac{W_r \bar{C}_{P_v} (1 - K)}{4 R_v KR_1} \right]} - 1 \right\}} \quad (32)$$

Equation (32) will provide  $W_r$  in terms of the inner oxide radius  $R_1$  and  $K$

$$\frac{W_r (1 - K)}{KR_1} = \frac{4\pi k_v}{\bar{C}_{p_v}} \ln \left[ \frac{\bar{C}_{p_v} (T_c - T_{BP})}{\Delta H_{vap}} + 1 \right] \quad (33)$$

It is possible to determine  $R_2$  f ( $R_1$ ,  $K$ ) from the mass burned and spherical geometry

$$R_o^3 - (KR_1)^3 \rho_m = (R_2^3 - R_1^2) \rho_1 \quad (34)$$

For small values of  $\Delta C$ , the equivalent rate of diffusion through the spherical oxide shell also gives the mass transfer and oxidation rates

$$W_r = \frac{4\pi D_{12} \Delta \bar{C}}{\frac{1}{R_1} - \frac{1}{R_2}} \quad (35)$$

The unique values of  $K$ ,  $R_1$ ,  $R_2$  and  $W_r$  exist where the mass transfer rates, from equations (33) and (35), are equal. A solution was made using a digital computer and Newton's method of solving the following equation for  $K$  based on equations (33) to (35).

$$f(K) = \frac{4\pi D_{12} \Delta C (1-K)}{K} + \left\{ \frac{R_m}{K} \left[ (R_o^3 - R_m^3) \frac{\rho_m}{\rho_i} + \left( \frac{R_m}{K} \right)^3 \right]^{-1/3} - 1 \right\} \\ \left\{ \frac{4\pi k_v}{\bar{C}_{P_v}} \ln \left[ \frac{\bar{C}_{P_v} (T_c - T_{BP})}{\Delta H_{vap}} + 1 \right] \right\} = 0 \quad (36)$$

The rate of heat generation by reaction at the oxide must equal the rate of heat transferred to the surroundings and to the metal sphere.

Because of the heat capacity of the oxide, the heat of reaction  $\Delta H_f$  decreases linearly with increasing temperature. This effect is small and calculations using reasonable estimates of the various oxide radii ( $R_o = 50$  microns) would require an oxide temperature  $T_c$  greater than the adiabatic flame temperature for aluminum, magnesium and beryllium if only this effect is considered. This means that  $\Delta H_f$  must be limited by a shift in the oxidation equilibrium or by partial vaporization of the oxide. The equilibrium constants for either type of reaction vary exponentially with temperature.

Once a temperature is reached where these effects cease to be negligible,  $\Delta H_f$  should decrease rapidly in one or more steps to zero at

the adiabatic flame temperature for the metal. In lieu of more precise data, the oxide temperature  $T_c$  is expected to approach the adiabatic flame temperature,  $T_A$ , for highly exothermic metal-oxygen systems. In the following calculations for each metal system, an arbitrary selection of the oxide temperature was made:  $T_c = T_A - 200^\circ\text{C}$ .

The evaluation is repeated for all selected values of  $R_m$ . The resultant oxidation rate,  $W_r$ , and associated values of  $R_m$  were used to determine the regression of the metal sphere radius versus time using

$$\frac{W_r}{\rho_m 4 \pi R_m^2} = \frac{-dR_m}{dt} \quad (37)$$

## Results

The results were machine computed and are plotted in Figures 6 and 7 for aluminum and beryllium respectively. The three curves in each figure represent three estimated values of  $D_{12} \Delta C$ ;  $10^{-4}$ ,  $10^{-5}$  and  $10^{-6} \text{ g sec}^{-1} \text{ cm}^{-1}$ . The computed elapsed times for combustion of 100 micron spheres are compared with the results from torch experiments in Table IV. The agreement with the estimated values of  $D_{12} \Delta C$  is excellent. The agreement confirms the selection of these orders of magnitude values for  $D_{12} \Delta C$ . If boiling points were reliably known at actual chamber pressures, an identical calculation using the proper boiling point for  $T_{BP}$  is expected to provide the elapsed time for combustion.

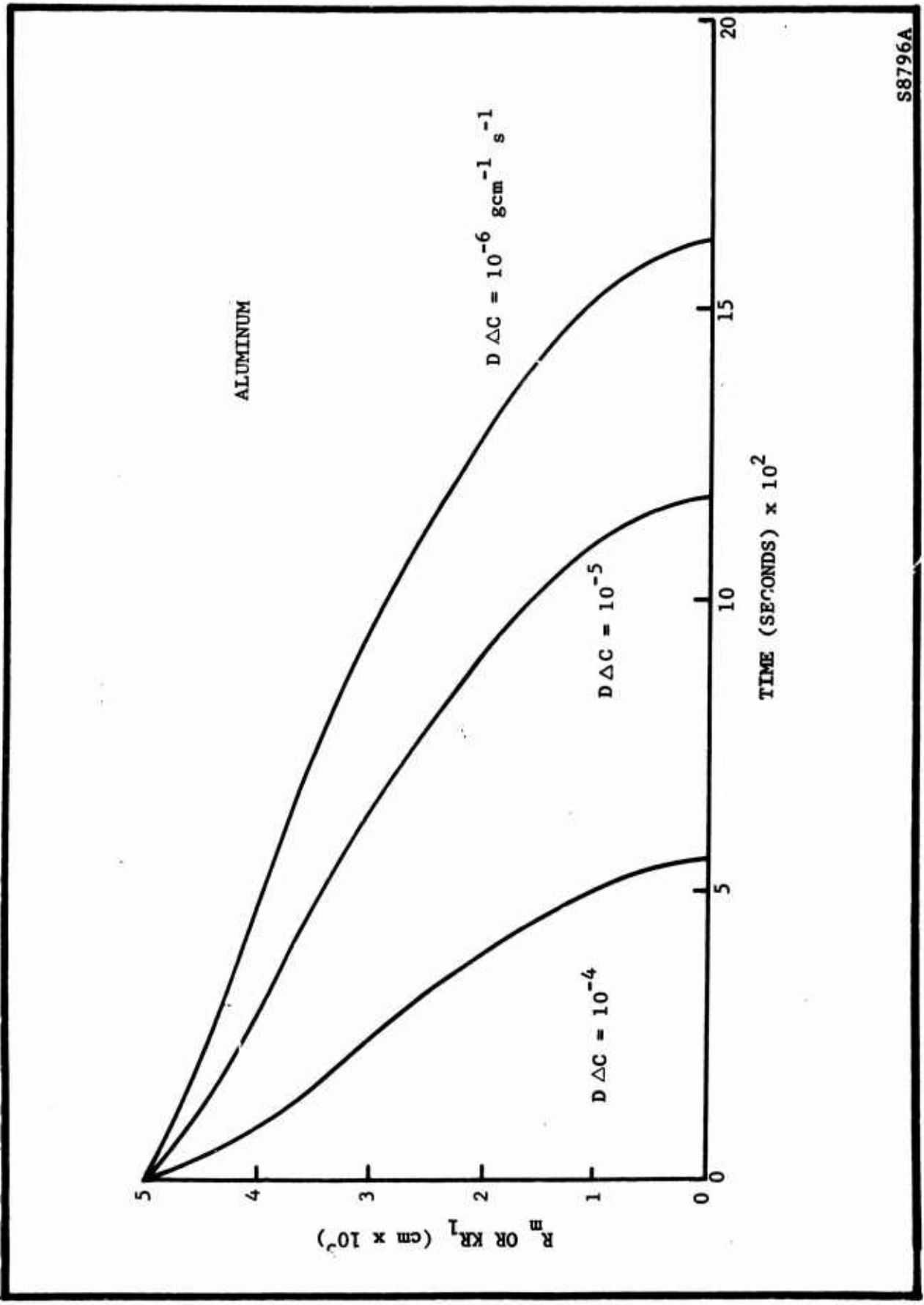
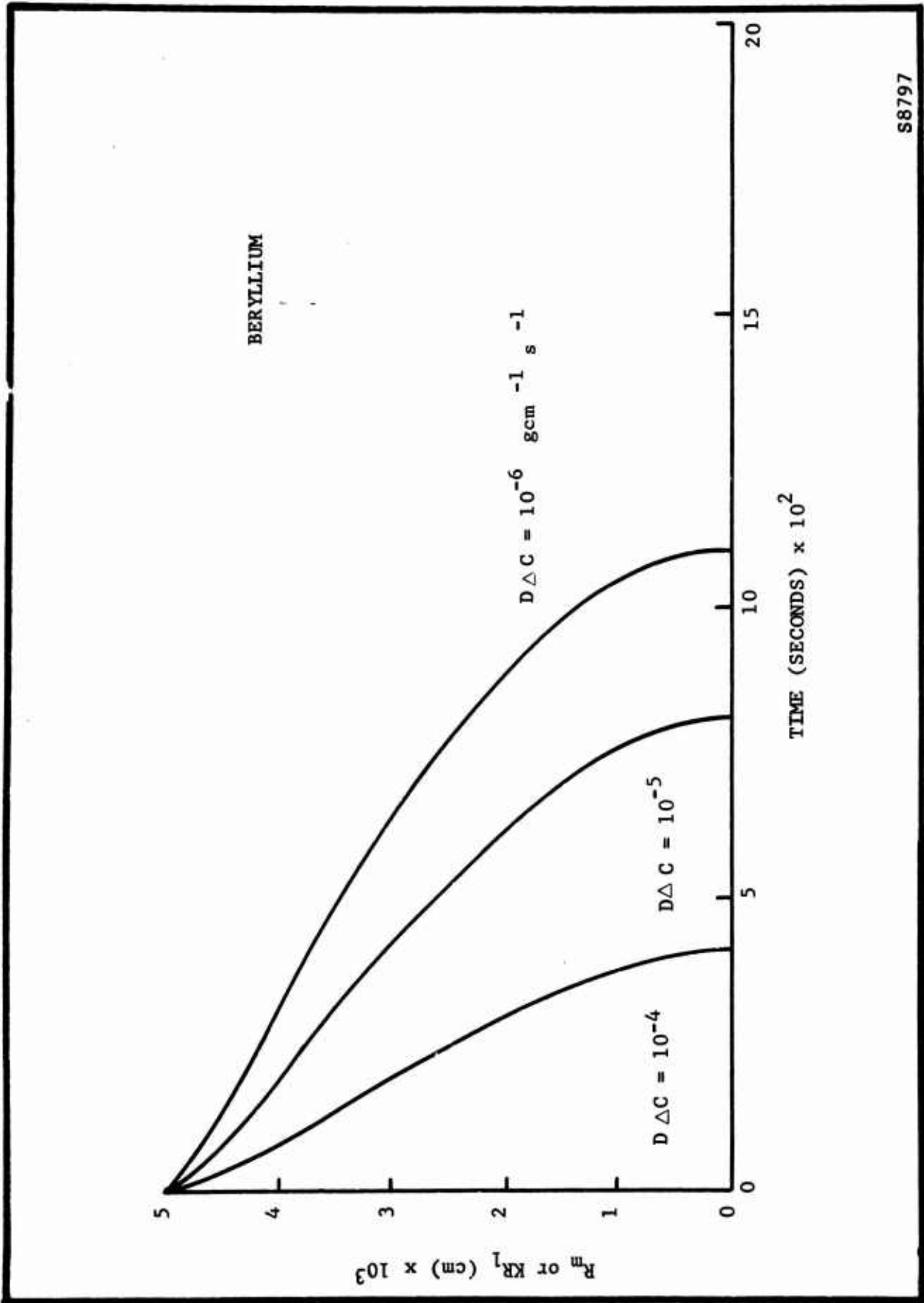


FIGURE 6. REGRESSION OF RADIUS DURING COMBUSTION OF 100-MICRON SPHERES OF ALUMINUM USING EVAPORATION MODEL; SYSTEM PRESSURE ONE ATMOSPHERE:  $T_A = 3700^\circ\text{K}$



S8797

FIGURE 7. REGRESSION OF RADIUS DURING COMBUSTION OF 100-MICRON SPHERES OF BERYLLIUM USING EVAPORATION MODEL; SYSTEM PRESSURE ONE ATMOSPHERE;  $T_A = 3900^\circ\text{K}$

TABLE IV

COMPARISON OF EXPERIMENTAL AND CALCULATED  
 COMBUSTION TIME (milliseconds) 100  $\mu$  ALUMINUM SPHERE

<u>Experimental</u>	<u>Calculated</u>	<u>Calculated</u>	<u>Calculated</u>
	$D_{12} \Delta C = 10^{-4}$	$D_{12} \Delta C = 10^{-5}$	$D_{12} \Delta C = 10^{-6}$
35-60	56	117	160

## DISCUSSION

The calculation of the elapsed times for the ignition delay and combustion periods requires specific knowledge of material constants at high temperatures which are not available and would be difficult to measure. The errors in estimating these values are contained in the final elapsed time calculation.

The unknown constant with the greatest effect on ignition delay is the thermal conductivity of the gas in the convective boundary film. The calculated results agree with experimental results within a factor of two and this discrepancy is within the probable error in the thermal conductivity.

The calculation of the combustion period is more hazardous, but errors in the diffusion coefficient-concentration difference product,  $D_{12} \Delta C$  exceed all others in significance. Errors in this product could conceivably amount to one or more orders of magnitude. The results for aluminum indicate  $D_{12} \Delta C$  is between  $10^{-4}$  and  $10^{-5}$  g cm<sup>-1</sup> sec<sup>-1</sup> which

seems reasonable, but an independent determination of this property is needed to verify the method of calculation. A considerable effort towards determining the diffusion coefficients of  $O^{2-}$  and the cations in fused oxides of aluminum and beryllium is needed. The desired information is useful in other fields including the reduction of metals, where transport through a slag phase is involved, and single phase ceramic technology.

## REFERENCES

1. S. S. Penner and B. P. Mullins, "Explosion, Detonations, Flammability and Ignition," Chap. VIII, p. 101, Pergamon Press, New York, (1959).
2. T. A. Brzustowski and I. Glassman, "Spectroscopic Investigation of Metal Combustion," Vol. 1, p. 203, Bulletin of the 17th meeting, JANAF-ARPA-NASA Solid Propellant Group, May, 1961.
3. A. V. Grosse and J. B. Conway, Ind. and Eng. Chem. Vol. 50, No. 4, p. 663, (1958).
4. A. W. Blackman and D. K. Kuehl, "The use of Binary Light Metal Mixtures and Alloys as Additives for Solid Propellants," ARS Solid Propellant Rocket Conference, Salt Lake City, Utah, February, 1961.
5. I. A. Vulis, "Thermal Regimes of Combustion," Chap. 3, McGraw-Hill Book Company, New York, (1961).
6. R. Friedman and A. Macek, "Combustion and Flame," Vol. 6, No. 1, p. 9, (1962).
7. W. M. Fassell, Jr., C. A. Papp, D. L. Hildenbrand and R. P. Sernka, "The Experimental Nature of the Combustion of Metal Powders," Solid Propellant Rocket Research, M. Summerfield, ed., p. 259-270, Academic Press, New York, (1960).
8. C. N. Cochran and W. Sleppy, Journal of Electrochemistry Society, Vol. 108, p. 322, (1961).
9. W. Bradshaw and E. S. Wright, "High Temperature Corrosion of Beryllium in Air," Lockheed Aircraft Corp, Navy Bureau of Weapons Contract NOrd 17017, AD 239 349, December, 1959.
10. S. Glasstone, K. S. Laidler and H. Eyring, "The Theory of Rate Processes," Chap. 9, McGraw-Hill Book Company, New York, (1941).
11. W. M. Fassell, Jr., L. B. Gulbransen, J. R. Lewis and J. H. Hamilton, Journal of Metals, Vol. 3, (1951).
12. T. E. Leontis and F. N. Rhines, Trans. AIME, Vol. 166, p. 265, (1946).

13. W. E. Ranz and W. R. Marshall, Jr., Chemical Engineering Progress, Vol. 48, pp. 141-146, 173-180, (1952).
14. J. O. Hirschfelder, D. F. Curtiss and R. B. Bird, "Molecular Theory of Gases and Liquids," Chaps. 8 and 9, John Wiley and Sons, New York, (1954).
15. W. D. Kingery, "Property Measurements at High Temperatures," p. 387, John Wiley and Sons, New York, (1959).
16. H. S. Carslaw and J. C. Jaeger, "Conduction of Heat in Solids," p. 242, Oxford Press, London, (1959).
17. W. Jost, "Diffusion in Solids, Liquids, Gases," p. 474, Academic Press, New York, (1960).